Identifying elastoplastic parameters with Bayes' theorem considering double error sources and model uncertainty

H. Rappel[a,b], L.A.A. Beex[a,*], L. Noels[b], S.P.A. Bordas[a,c]

[a] *Institute of Computational Engineering, Faculty of Science, Technology and Communication, University of Luxembourg, Maison du Nombre, 6, Avenue de la Fonte, 4364, Esch-sur-Alzette, Luxembourg.*
[b] *Computational & Multiscale Mechanics of Materials (CM3), Department of Aerospace and Mechanical Engineering, University of Liège, Quartier Polytech 1, Allée de la Découverte 9, B-4000 Liège, Belgium.*
[c] *School of Engineering, Cardiff University, Queen's Buildings, The Parade, Cardiff CF243AA, Wales, UK.*

Abstract

We discuss Bayesian inference for the identification of elastoplastic material parameters. In addition to errors in the stress measurements, which are commonly considered, we furthermore consider errors in the strain measurements. Since a difference between the model and the experimental data may still be present if the data is not contaminated by noise, we also incorporate the possible error of the model itself. The three formulations to describe model uncertainty in this contribution are: (1) a random variable which is taken from a normal distribution with constant parameters, (2) a random variable which is taken from a normal distribution with an input-dependent mean, and (3) a Gaussian random process with a stationary covariance function. Our results show that incorporating model uncertainty often, but not always, improves the results. If the error in the strain is considered as well, the results improve even more.

Keywords: Bayesian inference, Bayes' theorem, stochastic identification, parameter identification, elastoplasticity, plasticity, model uncertainty

1. Introduction

A frequent approach for the identification of material parameters in solid mechanics is the least squares method (LSM; see [1]), in which the squared difference between the experimental output and the model response is minimised with respect to the material parameters. The result of such an approach is a deterministic estimate of the parameter values. A true insight in the certainty of each identified parameter value lacks however, as only a single residual forms the measure for the quality of the ensemble of identified values. Although some advanced formulations of LSM incorporate statistical information [2, 3], they assume that the measurement error is symmetrically distributed. For nonlinear models furthermore, linearised approximations are required to estimate the parameter distributions [4].

An alternative identification method is the Bayesian approach which allows accounting for modelling uncertainty and the statistical noises of the experimental devices [5]. The result of Bayesian inference (BI) is a probability density function (PDF) as a function of the parameters of interest. This PDF is called the posterior distribution in Bayesian terminology. Once the posterior distribution is obtained, statistical summaries of the posterior such as mean, the value at which the posterior PDF is maximal (i.e. the 'maximum-a-posteriori-probability' or 'MAP' point) and the covariance matrix need to be evaluated. With the exception of a few cases, numerical frameworks need to be employed for this. Markov chain Monte Carlo (MCMC) techniques [6–9] are probably the most frequently employed approaches for sampling PDFs.

Bayesian inference (BI) was used in various previous studies to identify material parameters. The earliest work known to the authors is that of Isenberg [10], in which it was used to identify elastic parameters

*Corresponding author
Email address: lars.beex@uni.lu, l.a.a.beex@gmail.com (L.A.A. Beex)

in 1979. In other works, this framework was employed to identify elastic material parameters based on dynamic responses [11–13]. BI was also used to identify the elastic constants of composite laminates in [14–17]. Spatially varying elastic parameters were furthermore identified using BI by Koutsourelakis [18]. An introduction to identify Young's moduli employing Bayesian inference can be found in [19].

Elastoplastic parameters were also identified using BI. Parameters in linear elasticity-perfect plasticity were identified by Most [20], while Bayesian updating via a polynomial chaos expansion for an elastoplastic system was considered by Rosić et al. [21]. In addition to elastoplastic material models, Bayesian updating procedures were employed to identify material parameters of hysteretic models [22, 23] and other nonlinear material models such as viscoelasticity and creep [24–26].

In none of the aforementioned studies, the fact that the model itself may not be perfectly equipped to capture the experimental measurements was considered. A framework that can deal with this was nevertheless introduced by Kennedy and O'Hagan [27] in 2001, which is currently known as the 'KOH' framework and was employed in [18, 28–32]. Another issue that has received little attention in previous studies is that not only the output (e.g. the stress measurements) can be polluted by statistical noise, but the input as well (e.g. the strain measurements).

The aim of this study is to present a Bayesian identification framework for elastoplasticity that can treat uncertainties in both the output and the input, whilst also accounting for model uncertainty. The framework is constructed to deal with experimental data coming from monotonically increasing, uniaxial tensile tests. Output errors (the noise in the stress measurements) are commonly considered in identification approaches using BI, but input errors (i.e. the errors in the strains) seem to remain untreated in Bayesian identification approaches. They may be worthwhile to include, because of the use of the clamp displacement as a measure to derive strains often overestimates the measured strains due to slip in the clamps. Even if digital image correlation (DIC) is employed to determine strains, errors may be included due to the finite accuracy of (1) the applied pixel patterns, (2) the finite resolution of the images, and (3) the algorithms of the DIC software, which come with different user-selected parameters (such as the size of facets) and finite minimisation residuals.

Bayesian updating including uncertainties in both output and input was yet employed in [33] for linear dynamic systems and was aimed at identifying modal parameters. The framework uses the assumption that the posterior can be approximated as a Gaussian distribution at the MAP point, which may be considered as a limitation. Studies in other fields can also be found that treat two error sources [34–39], but those studies effectively employ linear regression.

The KOH framework to address model uncertainty was furthermore not employed in any of the aforementioned studies. Model uncertainty can be incorporated in several ways in the KOH framework. The simplest way is to describe it with a constant variable, which is to be identified [30]. One can also use a random variable and treat the parameters of the random variable's distribution as unknown parameters that need to be identified as well (and hence, they appear in the posterior) [30, 40]. Instead of incorporating a deterministic variable, one can include a function of which the parameters are deterministic [41]. One can also include a random variable and assume its distribution's parameters to be dependent on the input [40]. Model uncertainty can also be represented by a Gaussian process [27, 32, 42]. More information on different ways to incorporate model uncertainty can be found in [40].

In this contribution, we investigate the effect of three model uncertainty formulations (i.e. a correction of the uniaxial material response in terms of the strain from ideal elasticity or elastoplasticity equations) on the parameter identification in elasticity and elastoplasticity: (1) a random variable which is assumed to come from a normal distribution with constant parameters, (2) a random variable which is assumed to come from a normal distribution with a mean that depends on the input (i.e. the strain) and (3) a Gaussian process with a zero mean and a stationary covariance function. On top of that, we also investigate how the incorporation of the input error influences the results.

The structure of the paper is as follows. Section 2 briefly discusses the expressions of the considered material models for uniaxial, monotonic tension. In Section 3, the main concepts of Bayesian frameworks for parameter identification are presented. In Section 4, the employed model uncertainty functions are elaborated, including the corresponding likelihood functions. Section 5 presents the Bayesian approaches that

incorporate both the measurements errors in the stresses and in the strains, as well as the model uncertainty. Indicative results are presented in Section 6. The measurement data in this section are artificially generated, so that we can compare the identified parameter distributions with the true values. Finally, this contribution is closed with conclusions (Section 7).

Remark. *Throughout this paper bold capitals and symbols denote matrices and bold lower case letters and symbols are vectors or columns.*

2. Material models

In this section we present the stress-strain relations of the considered material models for monotonic uniaxial tensile tests. The material models presented in this section are: linear elasticity and linear elasticity with linear hardening.

2.1. Linear elasticity

In linear elasticity, the stress-strain relation is described fully linearly. This relation can be written as follows for uniaxial tension:

$$\sigma(\epsilon, \mathbf{x}) = E\epsilon, \tag{1}$$

where σ is the stress, ϵ is the strain and $\mathbf{x}$ is the vector containing the material parameters, which here only consists of Young's modulus E.

2.2. Linear elasticity-linear hardening

In a linear elastic-linear hardening material model, the elastic response is again described linearly in terms of the elastic strain. Plastic deformation occurs with linear work hardening when the stress reaches initial yield stress σ_{y0}. In other words, the stress continues to increase (linearly) when plastic deformation takes place. The stress-strain relation for this model during monotonic, uniaxial tension reads:

$$\sigma(\epsilon, \mathbf{x}) = \begin{cases} E\epsilon & \text{if } \epsilon \leq \frac{\sigma_{y0}}{E} \\ \sigma_{y0} + \frac{HE}{H+E}\left(\epsilon - \frac{\sigma_{y0}}{E}\right) & \text{if } \epsilon > \frac{\sigma_{y0}}{E} \end{cases}, \tag{2}$$

where H denotes the hardening modulus and hence, $\mathbf{x} = \begin{bmatrix} E & \sigma_{y0} & H \end{bmatrix}^T$.

3. Bayesian parameter identification

In this section some concepts of Bayesian inference are explained. First, a rather standard Bayesian framework for parameter identification is presented. Subsequently, we present a Bayesian approach that incorporates a generalised model error term in the KOH framework. The parametrised formulations for the employed model errors and their corresponding likelihood functions are presented in Section 4 in more detail.

3.1. Bayesian inference fundamentals

Let $\mathbf{y} = \begin{bmatrix} y_1 & \cdots & y_{n_m} \end{bmatrix}^T$ be a vector of n_m measurements and let $\mathbf{x}$ be a vector of n_p parameters which are to be identified. Using the Bayes' theorem, one can write:

$$\pi(\mathbf{x}|\mathbf{y}) = \frac{\pi(\mathbf{x})\pi(\mathbf{y}|\mathbf{x})}{\pi(\mathbf{y})}, \tag{3}$$

where $\pi(\mathbf{x})$ denotes the prior distribution (i.e. the PDF that represents one's assumed prior knowledge about the parameters, e.g. the fact that the Young's modulus cannot be smaller than zero), $\pi(\mathbf{y}|\mathbf{x})$ denotes the likelihood function (i.e. the PDF that measures the likelihood that measurements $\mathbf{y}$ are observed, given a set of parameter values $\mathbf{x}$), $\pi(\mathbf{x}|\mathbf{y})$ denotes the posterior distribution (i.e. the PDF that describes the chance

to obtain parameters $\mathbf{x}$, given the measurements $\mathbf{y}$) and $\pi(\mathbf{y})$ is called the evidence. As the measured data ($\mathbf{y}$) are already known and hence, $\mathbf{y}$ are not variables in the posterior ($\pi(\mathbf{x}|\mathbf{y})$), the evidence is a constant number ($\pi(\mathbf{y}) = C \in \mathbb{R}^+$) which is independent of the parameters. Consequently, Eq. (3) behaves as follows:

$$\pi(\mathbf{x}|\mathbf{y}) \propto \pi(\mathbf{x})\pi(\mathbf{y}|\mathbf{x}). \tag{4}$$

Since the statistical quantities of interest, such as the mean, covariance and MAP point, are the same for Eq. (3) as for Eq. (4), it is sufficient to deal with Eq. (4). Next, we will discuss likelihood function $\pi(\mathbf{y}|\mathbf{x})$ in the presence of a general model error term.

3.2. Likelihood function

In the KOH framework, the relation between a stress measurement and the model response is written as [40]:

$$y = \sigma_{\text{true}} + \omega_y, \tag{5}$$

with

$$\sigma_{\text{true}} = \sigma(\epsilon, \mathbf{x}) + d(\epsilon), \tag{6}$$

where ω_y denotes the error in the stress measurement (output error), which is considered to be a realisation from the PDF that we call here the stress noise distribution. Furthermore, d denotes the model uncertainty which can be assumed to be dependent on the input (i.e. strain ϵ here). Assuming that we know the form of the noise distribution, the likelihood function reads:

$$\pi(y|\mathbf{x}, \mathbf{x}_d, \mathbf{x}_{\omega_y}) = \pi_{\omega_y}(y - \sigma(\epsilon, \mathbf{x}) - d(\epsilon)), \tag{7}$$

where $\mathbf{x}_d$ denotes the parameter vector of the model uncertainty and $\mathbf{x}_{\omega_y}$ denotes the vector of parameters of the stress noise distribution. Often, the stress noise distribution is assumed to be a Gaussian distribution with $s^2_{\omega_y}$ variance and zero mean. Frequently, the parameters for both the model uncertainty (d) and the stress noise distribution (i.e. s_{ω_y} for the Gaussian distribution with zero mean) are unknown and consequently, they must also be identified, i.e. they appear as variables in the posterior. As uniaxial tensile tests are generally performed in well-controlled tensile testers of which the parameters the noise distribution of the load cell can be rather straightforwardly calibrated, we assume that the stress noise distribution and its parameters can be defined through a noise calibration process.

Using Eqs. (4) and (7), the posterior distribution for a single measurement can be written as:

$$\pi(\mathbf{x}, \mathbf{x}_d|y) \propto \pi(\mathbf{x})\pi(\mathbf{x}_d)\pi_{\omega_y}(y - \sigma(\epsilon, \mathbf{x}) - d(\epsilon)), \tag{8}$$

where $\pi(\mathbf{x})$ denote $\pi(\mathbf{x}_d)$ are the prior PDFs for the model parameters and the model uncertainty parameters, respectively. Clearly, we have assumed here that the probabilities of the model parameters and of the model uncertainty are independent ($\pi(\mathbf{x}, \mathbf{x}_d) = \pi(\mathbf{x})\pi(\mathbf{x}_d)$). Furthermore, $\pi(\mathbf{x}, \mathbf{x}_d|y)$ denotes the joint PDF for $\mathbf{x}$ and $\mathbf{x}_d$. For the case of n_m independent measurements, the final likelihood function is a product of the likelihood functions for each output y_i (coming with input ϵ_i):

$$\pi(\mathbf{y}|\mathbf{x}, \mathbf{x}_d) = \prod_{i=1}^{n_m} \pi_{\omega_y}(y_i - \sigma(\epsilon_i, \mathbf{x}) - d(\epsilon_i)). \tag{9}$$

Once the posterior is established, one can employ numerical sampling techniques to approximate the posterior's statistical summaries (e.g. mean value, MAP point or covariance matrix). In this contribution the adaptive Metropolis algorithm [43] is employed to sample the posterior. The algorithm is elaborated in Appendix A.

4. Model uncertainty

In Section 3, Bayesian inference for a general model uncertainty was discussed. In this section, we present the likelihood functions for the three formulations of model uncertainty ($d(\epsilon)$), see Eq. (6). As mentioned before, these three formulations are: (1) a random variable coming from a normal distribution with a constant mean and variance, (2) a random variable which comes from a normal distribution with a constant variance and a mean which is a polynomial function in terms of the input (the strain), and (3) a Gaussian random process with a stationary covariance function.

Important to realise again is that the stress noise distribution is described by a normal distribution with zero mean and $s^2_{\omega_y}$ variance, i.e. $\omega_y \sim N(0, s^2_{\omega_y})$. As mentioned before, we assume that s_{ω_y} is known (see Subsection 6.1).

4.1. Random variable coming from a normal distribution with constant parameters

In the first case, we describe the difference between the material model and the true response as realisations from a normal distribution with mean $\overline{d}$ and variance s^2_d, i.e. $N(\overline{d}, s^2_d)$. $\overline{d}$ and s^2_d are unknown and must be identified by the Bayesian updating process. Prior knowledge about them can be incorporated in the prior distribution. The likelihood function of for n_m measurements, previously expressed in Eq. (9), can now be written as:

$$\pi(\mathbf{y}|\mathbf{x}, \mathbf{x}_\mathrm{d}) = N(\boldsymbol{\sigma}(\boldsymbol{\epsilon}, \mathbf{x}) + \overline{d}\mathbf{1}_{n_m}, (s^2_{\omega_y} + s^2_\mathrm{d})\mathbf{I}_{n_m}), \tag{10}$$

where $\boldsymbol{\sigma}(\boldsymbol{\epsilon}, \mathbf{x})$ denotes the vector of model responses for each input $\begin{bmatrix}\sigma(\epsilon_1, \mathbf{x}) & \cdots & \sigma(\epsilon_{n_m}, \mathbf{x})\end{bmatrix}^T$, $\mathbf{1}_{n_m}$ denotes the unit vector of size $n_m \times 1$, $\mathbf{I}_{n_m}$ denotes the identity matrix of size $n_m \times n_m$ and $\mathbf{x}_d$ denotes the parameter vector for the model uncertainty i.e. $\mathbf{x}_d = \begin{bmatrix}\overline{d} & s_d\end{bmatrix}^T$. Eq. (10) clearly shows that this model uncertainty adds a correction to the mean and increases the likelihood's variance by s^2_d.

4.2. Random variable coming from a normal distribution with an input dependent mean

In the second case, we describe the difference between the model response and the true response as a random variable, that originates from a normal distribution of which the mean is a function of the input. We use polynomial functions to describe the relation between the mean and the input, $\overline{d}(\epsilon) = \sum_{l=0}^{L} a_l \epsilon^l$, resulting in $L+2$ model uncertainty parameters: $\mathbf{x}_d = \begin{bmatrix}a_0 & a_1 & \cdots & a_L & s_d\end{bmatrix}^T$. Consequently, the likelihood function reads:

$$\pi(\mathbf{y}|\mathbf{x}, \mathbf{x}_\mathrm{d}) = N(\boldsymbol{\sigma}(\boldsymbol{\epsilon}, \mathbf{x}) + \overline{\mathbf{d}}(\boldsymbol{\epsilon}), (s^2_{\omega_y} + s^2_\mathrm{d})\mathbf{I}_{n_m}), \tag{11}$$

where $\overline{\mathbf{d}}(\boldsymbol{\epsilon}) = \begin{bmatrix}\overline{d}(\epsilon_1) & \cdots & \overline{d}(\epsilon_{n_m})\end{bmatrix}^T$. Note that increasing the polynomial order can lead to model nonidentifiability [40].

4.3. Gaussian process with a stationary covariance function

In the work of Kennedy and O'Hagan [27], model uncertainty was described by a Gaussian process [44], entailing that the error between the model and the true response is nonlocal in terms of the strain (i.e. the input). Following [27] and [42] describing a Gaussian process (GP) with a zero mean, we write:

$$d \sim \mathrm{GP}(0, \lambda^2 c(\cdot, \cdot|\psi)), \tag{12}$$

where c is the squared exponential correlation function:

$$c(\epsilon_i, \epsilon_j|\psi) = \exp\Big(-\frac{(\epsilon_i - \epsilon_j)^2}{2\psi^2}\Big), \tag{13}$$

where λ^2 denotes the variance and ψ the length scale, yielding $\mathbf{x}_d = \begin{bmatrix}\lambda & \psi\end{bmatrix}^T$. ϵ_i and ϵ_j furthermore denote two input values which may be the same ($i, j \in \{1, \cdots, n_m\}$). Note that the zero mean in the Gaussian

process implies that no bias is included that increases the chance for $d(\epsilon)$ to be positive or negative. The likelihood function now reads:

$$\pi(\mathbf{y}|\mathbf{x}, \mathbf{x}_{\mathrm{d}}) = N(\boldsymbol{\sigma}(\boldsymbol{\epsilon}, \mathbf{x}), \boldsymbol{\Gamma}_{\mathrm{GP}} + s^2_{\omega_y} \mathbf{I}_{n_m}), \tag{14}$$

where

$$\boldsymbol{\Gamma}_{\mathrm{GP}} = \begin{bmatrix} \lambda^2 c(\epsilon_1, \epsilon_1|\psi) & \cdots & \lambda^2 c(\epsilon_1, \epsilon_{n_m}|\psi) \\ \vdots & \ddots & \vdots \\ \lambda^2 c(\epsilon_{n_m}, \epsilon_1|\psi) & \cdots & \lambda^2 c(\epsilon_{n_m}, \epsilon_{n_m}|\psi) \end{bmatrix}. \tag{15}$$

Eq. (15) clearly shows that the errors in the stress measurements are correlated in a GP. This implies that the updating procedure is not performed by a multiplication operator as in Eq. (9). Instead, we consider $\mathbf{y}$ to be a realisation from a multivariate Gaussian distribution with non-zero off-diagonal components (unlike the cases in Subsections 4.1 and 4.2, in which the covariance matrix of the likelihood function only has non-zero components on its diagonal).

5. Model uncertainty and noise in the strain

In the previous sections, we have assumed that the strain measurements are perfect (i.e. they are not polluted by noise). In this section, we reformulate the framework such that it can also treat errors in the strain. The errors in the stress and in the strain are assumed to be independent of each other, as the devices to measure the forces and strains or clamp displacements are independent of each other (e.g. if a load cell and digital image correlation are used). We first give the general likelihood function in case model uncertainty and the noise in the strain is incorporated (besides the commonly incorporated noise in the stress). Then, we specify the likelihood functions for the three material descriptions for monotonically increasing uniaxial tension, if only the error in the noise is incorporated. Subsequently, we include model uncertainty for the two material descriptions.

5.1. General likelihood function

In this subsection, a general likelihood function is presented that incorporates model uncertainty as well as the input error (and the output error obviously). As mentioned in Subsection 3.2, the experimental output in the KOH framework [27] can be written as follows:

$$y = \sigma(\epsilon, \mathbf{x}) + d(\epsilon) + \omega_y. \tag{16}$$

We now assume that each strain measurement, ϵ^*, is also polluted by some statistical error, ω_{ϵ^*}, in an additive manner:

$$\epsilon^* = \epsilon + \omega_{\epsilon^*}, \tag{17}$$

where ϵ is the true strain. Similar to the error in the stress measurements, we assume that the strain errors are realisations from a Gaussian distribution with a zero mean and variance $s^2_{\omega_{\epsilon^*}}$. Using Bayes' theorem, we can now write:

$$\pi(\mathbf{x}, \mathbf{x}_d, \epsilon|y, \epsilon^*) = \frac{\pi(y|\mathbf{x}, \mathbf{x}_d, \epsilon)\pi(\epsilon|\epsilon^*)\pi(\mathbf{x})\pi(\mathbf{x}_d)\pi(\epsilon^*)}{\pi(y|\epsilon^*)\pi(\epsilon^*)}, \tag{18}$$

or

$$\pi(\mathbf{x}, \mathbf{x}_d, \epsilon|y, \epsilon^*) \propto \pi(y|\mathbf{x}, \mathbf{x}_d, \epsilon)\pi(\epsilon|\epsilon^*)\pi(\mathbf{x})\pi(\mathbf{x}_d). \tag{19}$$

The joint distribution of the material parameter vector $\mathbf{x}$ and model uncertainty parameter vector $\mathbf{x}_d$ reads:

$$\pi(\mathbf{x}, \mathbf{x}_d|y, \epsilon^*) \propto \int_0^b \pi(y|\mathbf{x}, \mathbf{x}_d, \epsilon)\pi(\epsilon|\epsilon^*)d\epsilon\ \pi(\mathbf{x})\pi(\mathbf{x}_d), \tag{20}$$

where b denotes the physical upper bound of the tensile tester (i.e. the ratio of the original length of the specimen and the maximum distance that the clamps can displace). Assuming again that the noise distributions for both the stress and strain measurements are known, Eq. (20) reads:

$$\pi(\mathbf{x}, \mathbf{x}_d|y, \epsilon^*) \propto \int_0^b \pi_{\omega_y}(y - \sigma(\epsilon, \mathbf{x}) - d(\epsilon))\pi_{\omega_{\epsilon^*}}(\epsilon^* - \epsilon)d\epsilon\ \pi(\mathbf{x})\pi(\mathbf{x}_d), \tag{21}$$

where π_{ω_y} denotes the noise distribution for a stress measurement and $\pi_{\omega_{\epsilon^*}}$ denotes the noise distribution for a strain measurement. Note again that one may assume a form for both noise distributions and then treat the parameters of both distributions as unknowns, which are to be identified together with the material parameters and the model uncertainty parameters in the Bayesian updating procedure. However, we assume that these noise parameters can be identified using a separate calibration procedure (see Subsection 6.1).

For n_m measurements, the posterior reads:

$$\pi(\mathbf{x}, \mathbf{x}_d|\mathbf{y}, \boldsymbol{\epsilon}^*) \propto \underbrace{\int_0^b \cdots \int_0^b}_{n_m} \pi(\mathbf{y}|\mathbf{x}, \mathbf{x}_d, \boldsymbol{\epsilon})\pi(\boldsymbol{\epsilon}|\boldsymbol{\epsilon}^*)d\boldsymbol{\epsilon}\pi(\mathbf{x})\pi(\mathbf{x}_d), \tag{22}$$

where $\mathbf{y} = \begin{bmatrix} y_1 & \cdots & y_{n_m} \end{bmatrix}^T$, $\boldsymbol{\epsilon}^* = \begin{bmatrix} \epsilon_1^* & \cdots & \epsilon_{n_m}^* \end{bmatrix}^T$. We furthermore use now $\pi(\boldsymbol{\epsilon}|\boldsymbol{\epsilon}^*) = N(0, s_{\omega_{\epsilon^*}}^2 \mathbf{I}_{n_m})$. $\mathbf{I}_{n_m}$ denotes the identity matrix of size $n_m \times n_m$. In case of n_m independent measurements, the posterior reads:

$$\pi(\mathbf{x}, \mathbf{x}_d|\mathbf{y}, \boldsymbol{\epsilon}^*) \propto \prod_{i=1}^{n_m} \int_0^b \pi_{\omega_y}(y_i - \sigma(\epsilon, \mathbf{x}) - d(\epsilon))\pi_{\omega_{\epsilon^*}}(\epsilon_i^* - \epsilon)d\epsilon\ \pi(\mathbf{x})\pi(\mathbf{x}_d). \tag{23}$$

The integrals in Eqs. (20)-(23) are either numerically approximated (e.g. using Monte Carlo integration [45]) or analytically determined (see next subsection).

5.2. The likelihood function considering input error

5.2.1. Linear elasticity

In case of linear elasticity during monotonically increasing, uniaxial tension, Eq. (1) provides the model response, whilst the model uncertainty in Eq. (21) is ignored for now. Considering that $\omega_y \sim N(0, s_{\omega_y}^2)$ and $\omega_{\epsilon^*} \sim N(0, s_{\omega_y}^2)$, the likelihood function for a single measurement reads:

$$\pi(y|\mathbf{x}, \epsilon^*) = \frac{1}{2\pi s_{\omega_y} s_{\omega_{\epsilon^*}}} \int_0^b \exp\Big(- \Big[\frac{(y - E\epsilon)^2}{2s_{\omega_y}^2} + \frac{(\epsilon^* - \epsilon)^2}{2s_{\omega_{\epsilon^*}}^2} \Big] \Big) d\epsilon. \tag{24}$$

By computing the integral in Eq. (24) analytically, it can be rewritten as follows:

$$\pi(y|\mathbf{x}, \epsilon^*) = \frac{\sqrt{p_3}}{2\sqrt{2\pi} s_{\omega_y} s_{\omega_{\epsilon^*}}} \exp\Big(- \frac{p_2 - p_1^2}{2p_3} \Big) \Big[\mathrm{erf}\Big(\frac{b - p_1}{\sqrt{2p_3}} \Big) - \mathrm{erf}\Big(\frac{-p_1}{\sqrt{2p_3}} \Big) \Big], \tag{25}$$

where $\mathrm{erf}(\cdot)$ is the error function [46] and p_1, p_2 and p_3 are formulated as follows:

$$p_1 = \frac{E\, y s_{\omega_{\epsilon^*}}^2 + s_{\omega_y}^2 \epsilon^*}{E^2 s_{\omega_{\epsilon^*}}^2 + s_{\omega_y}^2},\ p_2 = \frac{s_{\omega_y}^2 (\epsilon^*)^2 + s_{\omega_{\epsilon^*}}^2 y^2}{E^2\ s_{\omega_{\epsilon^*}}^2 + s_{\omega_y}^2},\ p_3 = \frac{(s_{\omega_y} s_{\omega_{\epsilon^*}})^2}{E^2\ s_{\omega_{\epsilon^*}}^2 + s_{\omega_y}^2}. \tag{26}$$

In case of n_m measurements, $\pi(\mathbf{y}|\mathbf{x}, \boldsymbol{\epsilon}^*)$ is obtained using the product in Eq. (23).

5.2.2. Linear elasticity-linear hardening

For linear elasticity-linear hardening, the unknown parameters are $\mathbf{x} = \begin{bmatrix} E & \sigma_{y0} & H \end{bmatrix}^T$. Again substituting Eq. (2) in Eq. (21) results in the following likelihood function for a single measurement:

$$\pi(y|\mathbf{x},\epsilon^*) = \frac{1}{2\sqrt{2\pi}s_{\omega_y}s_{\omega_{\epsilon^*}}}\Bigg(\sqrt{p_3}\exp\Big(-\frac{p_2-p_1^2}{2p_3}\Big)\Big[\mathrm{erf}\Big(\frac{\frac{\sigma_{y0}}{E}-p_1}{\sqrt{2p_3}}\Big)-\mathrm{erf}\Big(\frac{-p_1}{\sqrt{2p_3}}\Big)\Big]+ \\ \frac{1}{\sqrt{p_1^*}}\exp\Big(-\frac{p_1^*p_3^*-p_2^{*2}}{2p_1^*}\Big)\Big[\mathrm{erf}\Big(\frac{\sqrt{p_1^*}a-\frac{p_2^*}{\sqrt{p_1^*}}}{\sqrt{2}}\Big)-\mathrm{erf}\Big(\frac{\frac{\sigma_{y0}\sqrt{p_1^*}}{E}-\frac{p_2^*}{\sqrt{p_1^*}}}{\sqrt{2}}\Big)\Big]\Bigg), \quad (27)$$

where p_1, p_2 and p_3 are again given by Eq. (26) and p_1^*, p_2^* and p_3^* are expressed as follows:

$$p_1^* = \frac{\left(\frac{HE}{H+E}\right)^2}{s_{\omega_y}^2}+\frac{1}{s_{\omega_{\epsilon^*}}^2},\ p_2^* = \frac{(y-\sigma_{y0})\frac{HE}{H+E}+\left(\frac{HE}{H+E}\right)^2\frac{\sigma_{y0}}{E}}{s_\sigma^2}+\frac{\epsilon^*}{s_{\omega_{\epsilon^*}}^2}, \\ p_3^* = \frac{(y-\sigma_{y0})^2+2(y-\sigma_{y0})\frac{HE}{H+E}\frac{\sigma_{y0}}{E}+\left(\frac{HE}{H+E}\right)^2\left(\frac{\sigma_{y0}}{E}\right)^2}{s_{\omega_y}^2}+\frac{(\epsilon^*)^2}{s_{\omega\epsilon^*}^2}. \quad (28)$$

In the following subsection we discuss the formulations of the likelihood functions if model uncertainty is incorporated as well.

5.3. The likelihood function considering input error and model uncertainty

Adding input-dependent model uncertainty renders even the likelihood function of the linear elastic material model impossible to analyse analytically. Consequently, we employ Monte Carlo integration to numerically approximate the integral of Eq. (20). $\pi(\mathbf{y}|\mathbf{x},\mathbf{x}_d,\boldsymbol{\epsilon})$ for all formulations of model uncertainty are given in Eqs. (10), (11) and (14).

Note that in the case of the GP, the components of the measurement vector $\mathbf{y}$ are correlated. This means that updating, according to the multiplication operation in Eq. (23), is not possible. Instead, we consider that measurement vector $\mathbf{y}$ is a realisation from a multivariant Gaussian distribution with non-zero off-diagonal components. In this case, Eq. (22) is used to construct the posterior.

6. Results

This section presents some examples of the Bayesian framework for the elastic and elastoplastic material models and uniaxial tensile data. The main points we aim to investigate are: (1) the influence of incorporating the input error, (2) the influence of incorporating the three types of model uncertainty and (3) the influence of incorporating both the input error and model uncertainty. (Naturally, the output error is considered in all results as well.)

For this purpose the measurements are generated numerically using responses which deviate from the constitutive responses. Next, Bayesian inference is used to identify the parameters of the material models given in Section 2. To investigate the effect of incorporating the input error and model uncertainty on the identification results, posteriors and posterior predictions (see Appendix B) are furthermore presented for various cases and compared with the true parameter values and measurements. However, we first start with the calibration of the two measurement noises for uniaxial tensile tests. Note that all results are obtained using the adaptive Metropolis method for 5×10^4 samples, whilst burning the first 1.5×10^4 samples.

6.1. Noise calibration

We start the noise calibration procedure by acquiring measurement data without the use of actual specimens. Stress-strain measurements as schematically presented in Fig. 1. They show that both noises can be represented as individual normal distributions with zero means and their own variances. In this contribution we have assumed $s_{\omega_y} = 0.01$ GPa and $s_{\omega_{\epsilon^*}} = 5\times10^{-5}$.

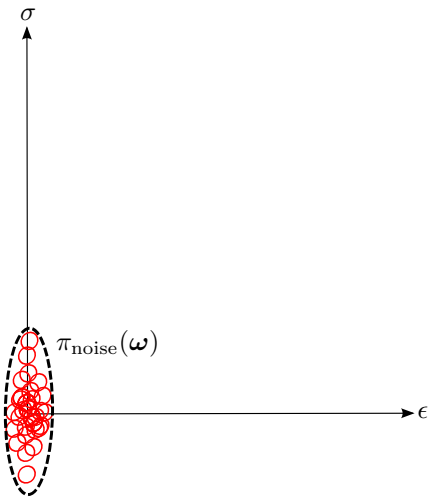

Figure 1: Schematic of the stress-strain measurements (red circles) of the 'noise calibration experiments', including an isoline if both noise distributions would be represented by a bivariate normal distribution (dashed).

6.2. Linear elasticity

6.2.1. Input error

In the first example, the added value of including the strain error is investigated for linear elasticity. The measurement data are generated using the following non-linear expression:

$$\sigma(\epsilon, a, E) = \frac{E\epsilon}{1 + \frac{\epsilon}{a}}, \tag{29}$$

where $E = 210$ GPa and $a = 0.015$. 20 measurements are generated using the same noise distributions as identified in the previous subsection. Parameter a in Eq. (29) is chosen such that the difference between the non-linear expression used to generate the measurements and its linear approximation in the neighbourhood of $\epsilon = 0$ (i.e. $\sigma = 210\epsilon$) is not too large (see Fig. 2(a)). We consider the following prior for the Young's modulus:

$$\pi(E) \propto \begin{cases} \exp\Big(- \frac{(E - \overline{E}_{\text{prior}})^2}{2 s^2_{\overline{E}_{\text{prior}}}} \Big) & \text{if } E \geq 0 \\ 0 & \text{otherwise} \end{cases}, \tag{30}$$

with $\overline{E}_{\text{prior}} = 150$ GPa and $s_{\overline{E}_{\text{prior}}} = 50$ GPa.

Fig. 2(b) presents the marginal posterior PDF of the Young's modulus for in case the output error alone is included (red curve) and for the case in which both the output and input errors are included (blue curve). Incorporating both error sources clearly results in a wider posterior. However, none of the resulting posteriors contains true value $E = 210$ GPa. The posterior mean and variance are given in Table 1.

The posterior predictions are shown in Fig. 3. One can observe that incorporating both error sources results in a wider envelope. This wider envelope includes more measurements, meaning that incorporating both error sources results in a more likely result.

6.2.2. Input error and model uncertainty

The effect of model uncertainty on the resulting posterior is studied now. First, we only include the case with output error but without input error. The prior used for the Young's modulus is the same mentioned

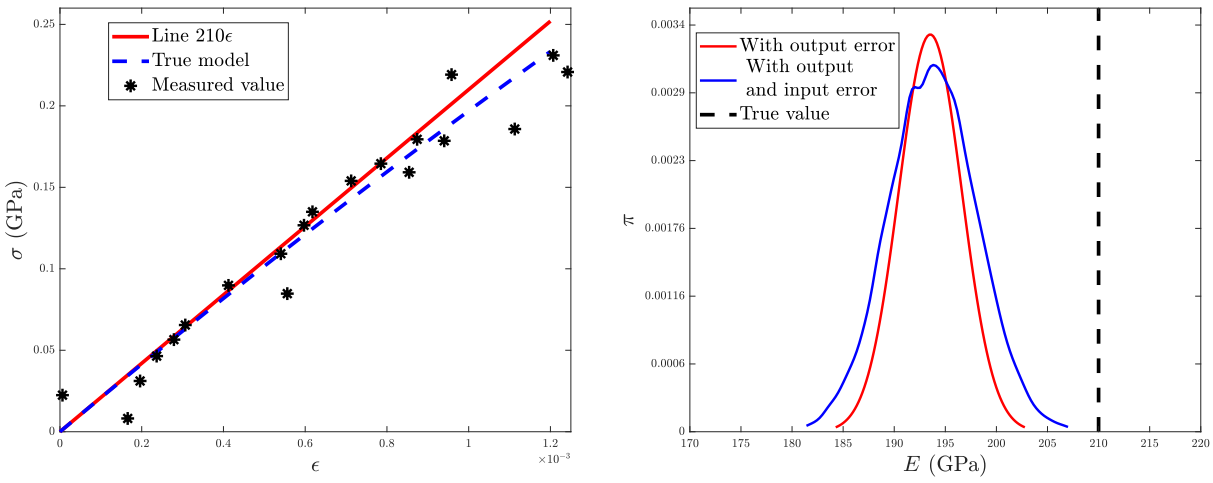

(a) (b)

Figure 2: Linear elasticity: (a) The experimental data generated for the first example, including the curve from which the data points are generated and its linearisation at $\epsilon = 0$. One can see that parameter a is chosen such that the difference between line 210ϵ and the true model is not large for small strains. (b) The marginal posterior PDF of the Young's modulus if the stress error alone is incorporated (red curve) and if the stress and strain errors are incorporated (blue curve). Considering both errors results in a wider distribution of the Young's modulus, but none of the distributions contain the true value.

previously. For the case in which model uncertainty is considered as a random variable coming from a Gaussian distribution with an input-dependent mean, we consider the following expression for its mean:

$$\overline{d}(\epsilon) = a_0 + a_1\epsilon + a_2\epsilon^2. \tag{31}$$

In case model uncertainty is modelled as a random variable, either coming from a Gaussian distribution with constant parameters or coming from a Gaussian distribution with an input-dependent mean, infinitely wide uniform distributions are used as prior distributions for the model uncertainty parameters ($\mathbf{x}_d$). However, for the case in which model uncertainty is described as a Gaussian process with a stationary covariance function, we have considered the following prior distributions for the model uncertainty parameters ($\mathbf{x}_d = \begin{bmatrix}\lambda & \psi\end{bmatrix}^T$):

$$\pi(\lambda) \propto \begin{cases} \exp\left(-\frac{(\lambda-\overline{\lambda}_{\text{prior}})^2}{2s^2_{\overline{\lambda}_{\text{prior}}}}\right) & \text{if } \lambda \geq 0 \\ 0 & \text{otherwise} \end{cases}, \tag{32}$$

and,

$$\pi(\psi) \propto \begin{cases} \exp\left(-\frac{(\psi-\overline{\psi}_{\text{prior}})^2}{2s^2_{\overline{\psi}_{\text{prior}}}}\right) & \text{if } \psi \geq 1.578 \times 10^{-5} \\ 0 & \text{otherwise} \end{cases}, \tag{33}$$

where $\overline{\lambda}_{\text{prior}} = 0.025$ GPa, $s_{\overline{\lambda}_{\text{prior}}} = 0.0083$ GPa, $\overline{\psi}_{\text{prior}} = 0.0006$ and $s_{\overline{\psi}_{\text{prior}}} = 0.0003$.

It must be noted that if infinitely wide uniform distributions are used for the model uncertainty parameters of the Gaussian process, the MCMC algorithm fails to converge. Using the fact that the model uncertainty function ($d(\epsilon)$) is a smooth function, we have chosen the mean of the prior for the length scale parameter ($\overline{\psi}_{\text{prior}}$) to be half of the maximum occurring strain. The standard deviation is chosen to be relatively large. To prevent negative length scale parameters and length scale parameters smaller than the minimum distance between two consecutive strains to be realised from the prior distribution, we have set a lower bound on the prior distribution. We have chosen the value of the mean of the variance of the GP ($\overline{\lambda}_{\text{prior}}$ in Eq. (32))

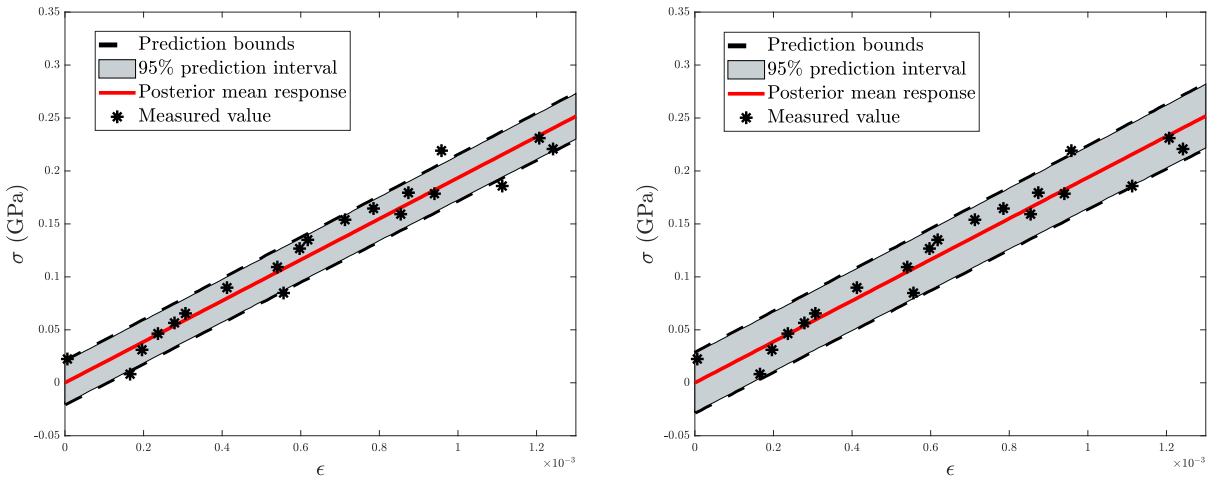

(a) Error in the stress measurements only

(b) Error in both the stress and strain measurements

Figure 3: Linear elasticity: The measurements, the posterior mean response and the posterior predictions. One can observe that the incorporation of both error sources results in a wider envelope, thereby including more measurements.

as 10% of the maximum occurring stress and the standard deviation such that 99.7% of the realisations coming from the prior distribution remain below 20% of the maximum occurring stress. A lower bound is also included (Eq. (32)).

Fig. 4(a) shows that the incorporation of model uncertainty increases the widths of the posteriors, such that the true value is possible to be generated from it. On the other hand, the MAP point (point estimator) when model uncertainty is not incorporated is closer to the true value than all the other posteriors' MAP points.

An important point to mention here is that in case model uncertainty is incorporated as a random variable coming from a normal distribution with an input-dependent mean, the marginal posterior PDF is approximately the same as the prior of the Young's. The reason for this is the linear term that is present in the input-dependent mean ($a_1\epsilon$ in Eq. (31)), which is also present in the model ($E\epsilon$). If we ignore the linear term and instead use the following expression for the input-dependent mean:

$$\overline{d}(\epsilon) = a_0 + a_2\epsilon^2, \tag{34}$$

we obtain the PDF presented in Fig. 4(b). The figure shows that the marginal posterior includes the true value of the Young's modulus. The MAP point has furthermore moved substantially closer to the true value. This can be caused by the fact that the true response (Eq. (29)) is not highly nonlinear and hence, its difference with the linear approximation (here $E\epsilon$) can be rather accurately described by the remaining terms of the Taylor expansion of the true model.

The posterior predictions for the three kinds of model uncertainty are presented in Figs. 5(a), 5(c) and 5(e). The diagrams show that if model uncertainty is considered as a random variable coming from a normal distribution, either with constant parameters or an input-dependent mean, more measurements are included in the envelope than if model uncertainty is represented by a Gaussian process. By comparing Figs. 3 and 5(e) furthermore, it becomes clear that more measurement data is present in the posterior prediction's envelope if both errors in the stress and strain are considered than if model uncertainty is considered as a Gaussian process without input error. This can be caused by the fact that, although the posterior is wider, the mean and MAP point are further from the true value if model uncertainty is described by a Gaussian process (see Fig. 4(a) and Table 1).

The effect of treating the input error as well as incorporating model uncertainty is presented in Fig. 6 for the marginal posteriors. Note that we have used the same priors as before. One can see that the posteriors

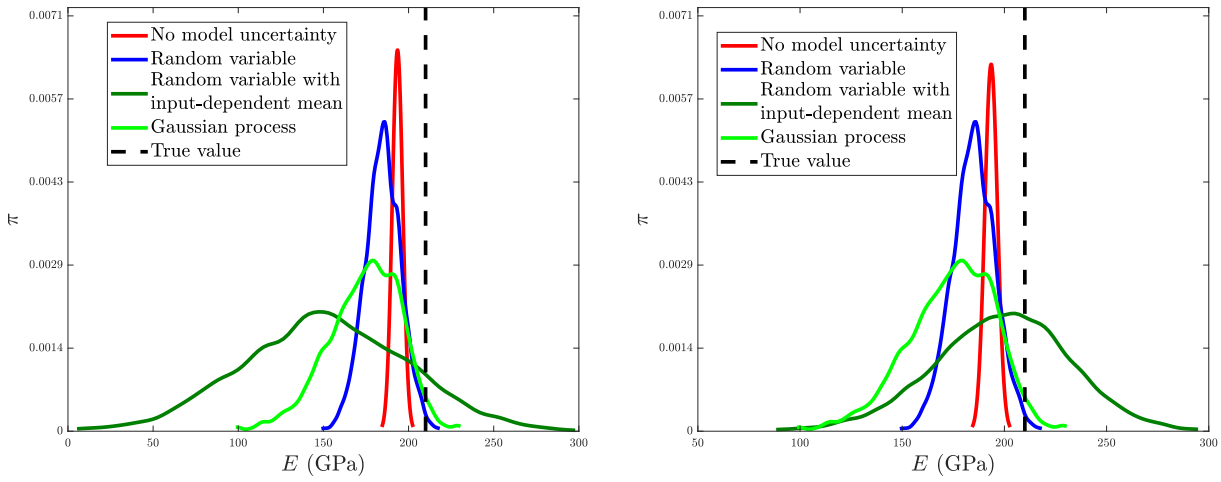

Figure 4: Linear elasticity: Marginal posteriors for the Young's modulus for different types of model uncertainty. (a) The mean for model uncertainty as a random variable coming from a Gaussian distribution with input-dependent mean, is given by Eq. (31). One can observe that incorporating any of the model uncertainties results in wider posterior distributions. Although the MAP point moves further away from the true value for all model uncertainty cases, all their posteriors include the true value, whereas the posterior for the case without model uncertainty does not include the true value. It must furthermore be noted that the posterior for the case in which model uncertainty is treated as a random variable coming from a Gaussian distribution with an input-dependent mean, is practically the same as the prior of the Young's modulus. (b) The same marginal posteriors as in (a), except that the case in which model uncertainty is modelled as a random variable coming from a normal distribution with an input-dependent mean, Eq. (34) is used for the mean instead of Eq. (31). One can see that the MAP point has moved considerably closer to the true value. This can be caused by the fact that the true stress-strain behaviour given in Eq. (29) is not highly nonlinear and the difference between $\sigma(\epsilon, a, E)$ in Eq. (29) and linear elasticity ($E\epsilon$) can rather accurately be represented by the remaining terms of a Taylor expansion for $\sigma(\epsilon, a, E)$.

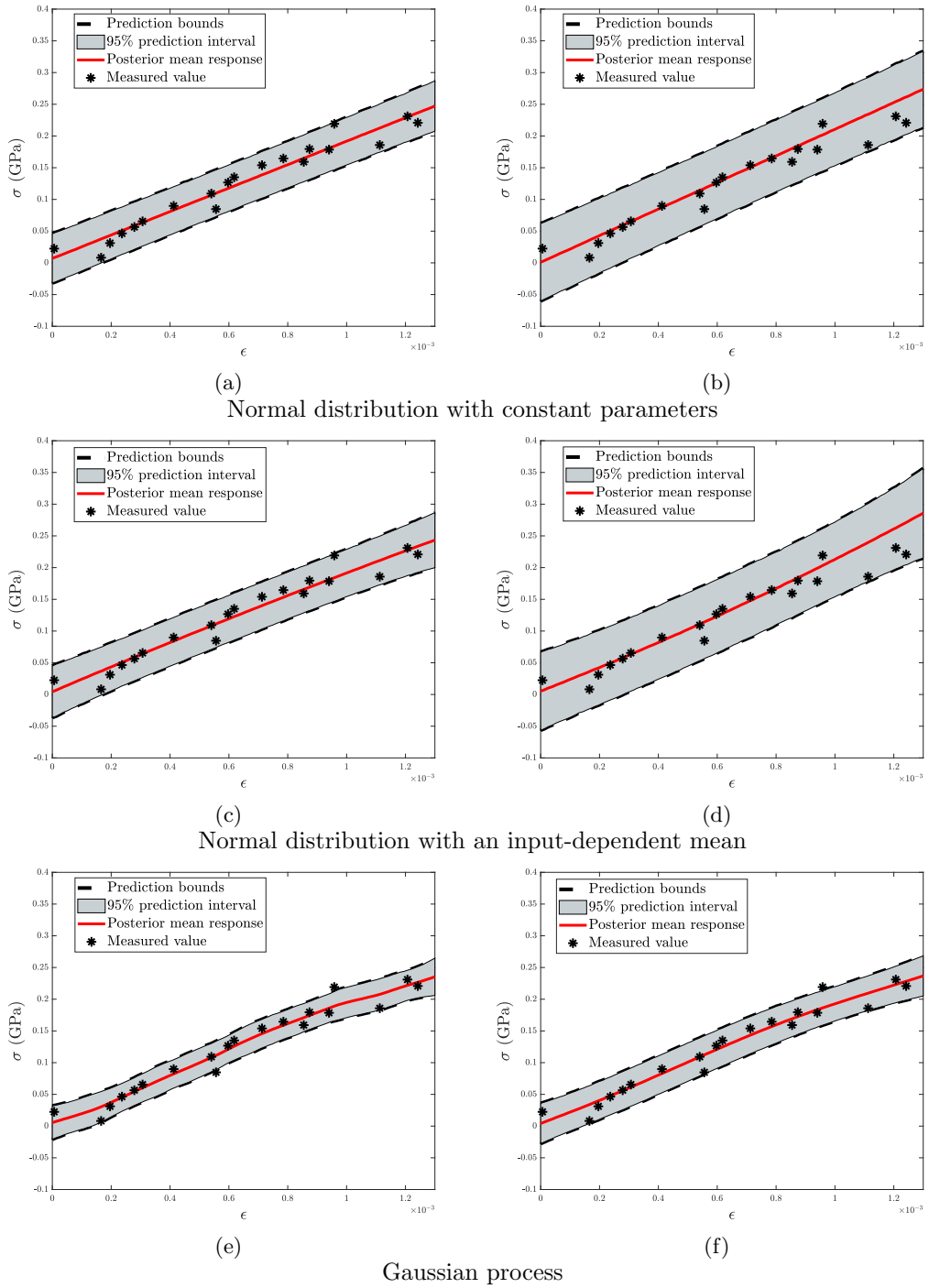

Figure 5: Linear elasticity: The measurements, the posterior mean responses and the posterior predictions. Left: without input error and right: including input error. One can see that if model uncertainty is described by a random variable coming from a normal distribution either with constant parameters or an input-dependent mean, more measurements are present inside the posterior's predictions interval than if a Gaussian process is considered. In case model uncertainty is a Gaussian process furthermore, one can see that including the input error results in more measurements to be present inside the posterior prediction bounds (cf. Figs. 5(e) and 5(f)).

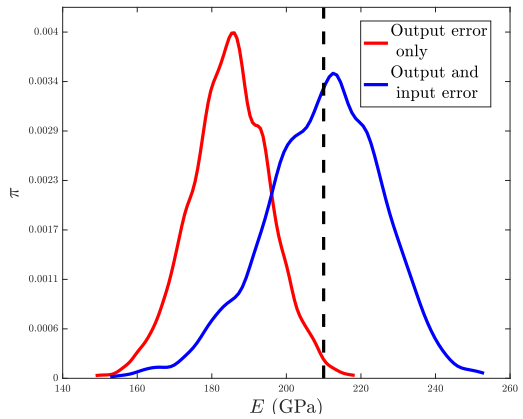

(a) Normal distribution with constant parameters

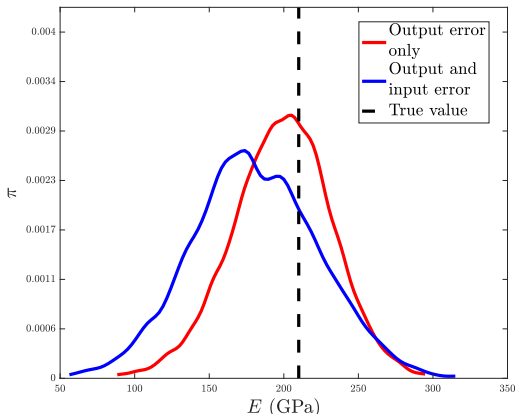

(b) Normal distribution with an input-dependent mean

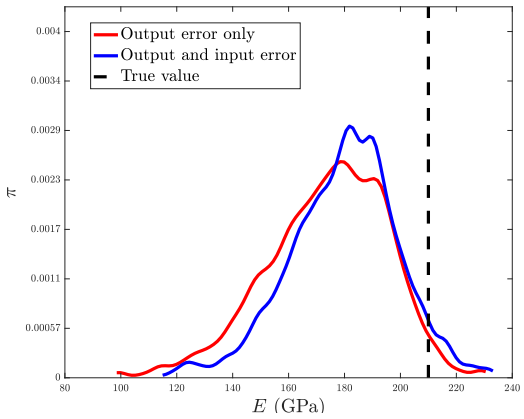

(c) Gaussian process

Figure 6: Linear elasticity: Marginal posteriors of the Young's modulus for three kinds of model uncertainty including input error. One can see that if model uncertainty is described by a random variable coming from a normal distribution (either with constant parameters or an input-dependent mean) the marginal posterior becomes wider if the input error is incorporated. In case model uncertainty is represented by a Gaussian process, the marginal posterior gets slightly narrower.

become wider if the input error is incorporated, except for the Gaussian process. That posterior has however changed such that the true value is less in its tail, than if the input error is not incorporated.

The posterior predictions for all three model uncertainties if the input error is also considered are shown in Figs. 5(b), 5(d) and 5(f). One can see that for both cases in which model uncertainty is a random variable, the posterior mean responses move closer to the measurement data. In case model uncertainty is considered as a Gaussian process, including the input error results in a wider envelope that includes more data (cf. Figs. 5(e) and 5(f)). Also the only data point not present in the envelope is still closer to the envelope if the input error is considered. The numerical values for the marginal posteriors mean, MAP point and standard deviation are given in Table 1.

6.3. Linear elasticity-linear hardening

For linear elasticity, we have shown that considering the error in the strain and model uncertainty leads to wider marginal posteriors of the Young's modulus (except if model uncertainty is treated as a Gaussian process). This can generally be considered as an improvement, because either the true value was present inside the wider distributions or the MAP point has moved towards the true value. For this case we have

Table 1: Linear elasticity: The numerical values of the mean, the MAP point and the standard deviation of the marginal posterior PDFs of the Young's modulus for all considered cases.

Model uncertainty	Mean (GPa)	MAP (GPa)	Standard deviation (GPa)
Error in the stress only			
None	193.5201	193.5201	3.0861
Random variable from a normal distribution with constant parameters	184.7892	185.6223	10.7162
Random variable from a normal distribution with an input-dependent mean	198.3326	209.6297	33.5192
Gaussian process with a stationary covariance function	173.8981	191.6519	21.5282
Error in the stress and strain			
None	193.7848	193.6629	4.3032
Random variable from a normal distribution with constant parameters	209.7249	208.3623	15.9041
Random variable from a normal distribution with an input-dependent mean	180.6751	187.1383	42.6510
Gaussian process with a stationary covariance function	179.6355	184.3772	19.4364

generated the data using relations that are not too different from the model response of interest. This has allowed us to compare the identified distributions with the true values. However, the measurement data may deviate considerably more from the model response. In this subsection, we present examples for linear elasticity-linear hardening. Because the deviation between the curves used to generate the data and the model response is so significant, we will not be able to compare the distributions with true values. Instead, we will only investigate the posterior predictions. We have initially generated 30 measurements using the following curve:

$$\sigma(\epsilon, a, \epsilon_{\max}) = a\sqrt{\epsilon_{\max}^2 - (\epsilon_{\max} - \epsilon)^2}, \tag{35}$$

where $a = 50$ GPa, $0 \leq \epsilon \leq \epsilon_{\max}$ and $\epsilon_{\max} = 0.0056$. Similar as in the previous subsection, output and input noise was generated using $s_{\omega_y} = 0.01$ GPa and $s_{\omega_{\epsilon^*}} = 5 \times 10^{-5}$ (see Fig. 7 for the measurements). The linear elastic-linear hardening model is used as the material description. This entails that we want to identify Young's modulus E, initial yield stress σ_{y0} and hardening modulus H. The same prior distribution as in Eq. (30) is used for the Young's modulus with $\overline{E}_{\text{prior}} = 100$ GPa, $s_{\overline{E}_{\text{prior}}} = 50$ GPa. The prior for the yield stress and the hardening modulus read:

$$\pi(\sigma_{y0}) \propto \begin{cases} \exp\Big(- \frac{(\sigma_{y0} - \overline{\sigma}_{y0_{\text{prior}}})^2}{2s^2_{\overline{\sigma}_{y0_{\text{prior}}}}} \Big) & \text{if } \sigma_{y0} \geq 0 \\ 0 & \text{otherwise} \end{cases}, \tag{36}$$

and

$$\pi(H) \propto \begin{cases} \exp\Big(- \frac{(H - \overline{H}_{\text{prior}})^2}{2s^2_{\overline{H}_{\text{prior}}}} \Big) & \text{if } H \geq 0 \\ 0 & \text{otherwise} \end{cases}, \tag{37}$$

where $\overline{\sigma}_{y0_{\text{prior}}} = 0.25$ GPa, $s_{\overline{\sigma}_{y0_{\text{prior}}}} = 0.025$ GPa, $\overline{H}_{\text{prior}} = 30$ GPa and $s_{\overline{H}_{\text{prior}}} = 15$ GPa. In case model uncertainty is described by a random variable coming from a normal distribution with an input-dependent mean, the relation of Eq. (31) is used for the mean. Furthermore, the prior distributions of the covariance function's parameters for the Gaussian process are given in Eqs. (32) and (33) with $\overline{\lambda}_{\text{prior}} = 0.03$ GPa, $s_{\overline{\lambda}_{\text{prior}}} = 0.01$ GPa, $\overline{\psi}_{\text{prior}} = 0.0028$ and $s_{\overline{\psi}_{\text{prior}}} = 9.3333 \times 10^{-4}$. The lower limit for length scale parameter ψ is set to 2.5×10^{-5}.

The posterior predictions are presented in Fig. 7. Two main issues can be observed. (1) By comparing Figs. 7(a) and 7(b), it can be noticed that including the error in the strain results in a wider prediction interval. This is especially true for the initial part of the response in which the model response is only governed by elasticity. This is due to the fact that the Young's modulus is larger than the stiffness during elastoplastic deformation (i.e. $\frac{HE}{H+E}$ in Eq.(2)). (2) Considering model uncertainties furthermore results in wide posterior prediction envelopes, which consequently include almost all measurement and verification points. Only for the case in which model uncertainty is represented by a random variable coming from a normal distribution with constant parameters, two verification points are not present within the bounds. One should note however, that in the cases in which model uncertainty is input-dependent, the model uncertainty is so dominant that the two linear regimes in the model response (the elastic regime and the elastoplastic regime) cannot be recognised anymore.

It is also worth to mention that in case the difference between the constitutive model (here linear elasticity-linear hardening) and the true response used to generate the measurements (here Eq. (35)) is large, the influence of incorporating model uncertainty is larger than that of incorporating the error in the strain. Incorporating the error in the strain, if model uncertainty is to be incorporated, can still have a positive influence however, as we have presented for linear elasticity.

In the examples in which linear elasticity were considered, we were able to compare not just the posterior predictions with the measurement data, but also the marginal posteriors with the true values. In case of linear elasticity-linear hardening, it is not possible to compare the marginal posteriors with the true values, because the material model and the true response do not share any parameters. In the case of linear elasticity-linear hardening therefore, we have introduced and will introduce verification points in order to compare the posterior predictions in more detail. In Fig. 7, we have shown verification points inside the domain of the measured strains. Now, we will add verification data outside the strain domain and investigate the posterior predictions for the verification points outside the initial strain domain.

Instead of 30 measurements, we now consider 20 measurements, polluted by noise coming from the aforementioned noise distributions. All priors and their parameters remain the same, except that the covariance function's parameters for the Gaussian process are set to $\overline{\lambda}_{\text{prior}} = 0.026$ GPa, $s_{\overline{\lambda}_{\text{prior}}} = 0.0087$ GPa, $\overline{\psi}_{\text{prior}} = 0.0018$ and $s_{\overline{\psi}_{\text{prior}}} = 0.0006$. The lower limit for length scale parameter ψ is set to 2.5×10^{-5}.

The posterior predictions are shown in Fig. 8, together with the measurement and verification data. It can be observed that all verification data are inside the posterior predictions' bounds if model uncertainty is described by a random variable coming from a normal distribution with constant parameters or by a Gaussian process. In case model uncertainty is described by a Gaussian process furthermore, the uncertainty is substantially larger than if a random variable coming from a normal distribution with constant parameters is used. This can be due to the fact that the Gaussian process assumes the measurements to be correlated, and hence, the larger the distance from the measured data, less information is available and a larger spread is observed. It can furthermore be observed that the smallest number of verification data is present inside the posterior prediction's bounds if model uncertainty is represented by a normal distribution with an input-dependent mean. It must be noted though, that if another relation for the mean would be selected, the posterior predictions would differ.

7. Conclusions

In this contribution, we have formulated a Bayesian approach that considers the output error (the error in the stress), the input error (the error in the strain) and the uncertainty of the model in order to identify parameters in elasticity and elastoplasticity from monotonically increasing uniaxial tensile tests. We have

treated three types of model uncertainty: (1) a random variable coming from a normal distribution with constant parameters, (2) a random variable coming from a normal distribution with an input-dependent mean and (3) a Gaussian process with a stationary covariance function.

We have applied the identification approach to linear elasticity and linear elasticity-linear hardening. The measurement data were artificially generated, allowing us to compare the parameter distributions with the true values for linear elasticity because the material models and the true responses, used to generate the measurement data, shared parameters. For linear elasticity-linear hardening the difference between the true response, used to generate the measurement data, and the material model response was so significant that no parameters were shared by the two. Consequently, we have only used posterior predictions to assess the quality of the results.

The results for linear elasticity show that incorporating any of the three model uncertainty formulations results in wider marginal posterior distributions of the Young's modulus. Consequently, the chance that the posterior distributions include the true value increases. Incorporating model uncertainty also results in wider posterior prediction intervals, which therefore contain more measurements.

If, in addition to model uncertainty, the error in the strain is also incorporated, the marginal posterior (distribution) of the Young's modulus becomes even wider. The exception is the case in which model uncertainty is described by a Gaussian process (with a stationary covariance function). The posterior becomes narrower in this case, but the evaluation of the posterior at the true value is nevertheless larger. In other words, the true value has a higher chance to be realised from the posterior.

Incorporating the error in the strain (input error), as well as model uncertainty, also results in wider posterior prediction intervals, which are therefore more likely to contain the measurement data. If model uncertainty is described by a Gaussian process however, the posterior prediction interval does not become wider, but still contains more measurements than if the input error is not included.

Our results generally show that incorporating both model uncertainty and the input error has a favourable influence on the identified parameters and the posterior predictions, compared to only incorporating model uncertainty or only incorporating the input error. If the difference between the true response (used to generate the measurements) and the response of the material model increases however, the added value of incorporating the input error as well reduces substantially.

Acknowledgements

The authors would like to acknowledge the financial support from the University of Luxembourg and the European Research Council Starting Independent Research Grant (ERC Stg grant agreement No. 279578) entitled "Towards real time multiscale simulation of cutting in nonlinear materials with applications to surgical simulation and computer guided surgery".

Appendix A. Markov chain Monte Carlo (MCMC)

Markov chain Monte Carlo (MCMC) techniques are frequently employed numerical approaches to explore posteriors [45, 47], when they are too complex to be analytically analysed. Below, the Monte Carlo method and the adaptive Metropolis algorithm are discussed as means to explore the posterior PDF.

Appendix A.1. Monte Carlo principle

Consider that n_s samples are drawn from a PDF of interest that we denote by π_{post} (for the case mentioned above, $\pi_{\text{post}} = \pi(\mathbf{x}, \mathbf{x}_d|\mathbf{y})$). Then, the following integral can be approximated by averaging the values of function $\mathbf{f}(\mathbf{x})$ for the drawn n_s samples.

$$\widehat{\mathbf{f}}_{\text{int}} = \frac{1}{n_s}\sum_{i=1}^{n_s}\mathbf{f}(\mathbf{x}_i) \approx \int_{\mathbb{R}^{n_p}}\mathbf{f}(\mathbf{x})\pi_{\text{post}}(\mathbf{x})d\mathbf{x}, \tag{A.1}$$

where $\{\mathbf{x}_i\}_i^{n_s}$ is the finite set of samples drawn from π_{post}. From here onwards, we use hats on top of letters and symbols to denote their numerical approximations. Using the Monte Carlo principle, posterior's mean

$\widehat{\overline{\mathbf{x}}}_{\text{post}}$, MAP point $\widehat{\mathbf{MAP}}$ and the component of the posterior's covariance matrix at the j^{th} row and l^{th} column can be approximated as follows [45]:

$$\widehat{\overline{\mathbf{x}}}_{\text{post}} = \frac{1}{n_s}\sum_{i=1}^{n_s}\mathbf{x}_i, \tag{A.2}$$

$$\widehat{\mathbf{MAP}} = \underset{\mathbf{x}_i; i=1,\ldots,n_s}{\text{argmax}}\ \pi(\mathbf{x}_i), \tag{A.3}$$

and

$$(\widehat{\text{cov}}_{\text{post}})_{jl} = \frac{1}{n_{s-1}}\sum_{i=1}^{n_s}\Big((x_i)_j - (\widehat{\overline{x}}_{\text{post}})_j\Big)\Big((x_i)_l - (\widehat{\overline{x}}_{\text{post}})_l\Big),\ j = 1, 2, \cdots, n_p,\ l = 1, 2, \cdots, n_p. \tag{A.4}$$

Appendix A.2. The adaptive Metropolis algorithm

The Metropolis-Hastings [45] method is a frequently employed Markov chain Monte Carlo (MCMC) approach. In case a symmetric proposal is used, the algorithm is commonly referred to as a Metropolis algorithm.

The Metropolis algorithm explores the posterior PDF by a random walk in the parameter space $\mathbf{x}$. We consider sample $\mathbf{x}_i$ and the evaluation of the PDF of interested at this sample $\pi_{\text{post}}(\mathbf{x}_i)$. New sample $\mathbf{x}_p$ is then proposed by drawing from proposal distribution $q(\mathbf{x}_p|\mathbf{x}_i)$. If the PDF of interest at the proposed sample ($\pi_{\text{post}}(\mathbf{x}_p)$) is larger than its value at the current sample ($\pi_{\text{post}}(\mathbf{x}_i)$), the proposed sample is always accepted (this is correct if the proposal distribution in the Metropolis-Hastings algorithm is symmetric which is the case in the Metropolis algorithm). If $\pi_{\text{post}}(\mathbf{x}_p) < \pi_{\text{post}}(\mathbf{x}_i)$ however, the proposed sample may be accepted as the new sample. This depends on ratio r in Algorithm 1. If the proposed sample is rejected, the old sample is taken as the new sample. The algorithm is repeated for many samples and post-processing, in which the evolution of the statistical summaries is investigated, must point out if convergence is achieved.

The conventional Metropolis algorithm has the disadvantage that proposal distribution's parameters $q(\mathbf{x}_p|\mathbf{x}_i)$ must be manually tuned. Consequently, an adaptive variant was introduced by Haario et al. [43] in order to avoid this issue. The parameters of the proposal distribution are updated based on the knowledge about the posterior, harvested from the previous samples. We update the proposal distribution once every 1000 samples.

Often, a Gaussian distribution is used as a symmetric proposal distribution. In the adaptive Metropolis algorithm, this reads as:

$$q(\mathbf{x}_p|\mathbf{x}_i) = N(\mathbf{x}_i, \gamma^2\mathbf{R}), \tag{A.5}$$

where $\gamma^2\mathbf{R}$ denotes a covariance matrix of size $n_p \times n_p$, with n_p as the number of unknown parameters and hence, the number of dimensions of the posterior. γ must be selected initially and matrix $\mathbf{R}$ is updated based on the previous samples. We use the following initial value $\gamma = \frac{2.38}{\sqrt{n_p}}$, proposed by Gelman et al. [48]. Matrix $\mathbf{R}$ is established by storing all $n_{\mathbf{K}}$ previous samples in matrix $\mathbf{K}$ of size $n_{\mathbf{K}} \times n_p$. $\mathbf{R}$ is then computed as follows:

$$\mathbf{R} = \frac{1}{n_{\mathbf{K}} - 1}\widetilde{\mathbf{K}}^T\widetilde{\mathbf{K}}, \tag{A.6}$$

where $\widetilde{\mathbf{K}} = \mathbf{K} - \mathbf{K}_{\text{mean}}$ and $\mathbf{K}_{\text{mean}}$ reads:

$$\mathbf{K}_{\text{mean}} = \begin{bmatrix}\mathbf{k}_{\text{mean}}\\ \mathbf{k}_{\text{mean}}\\ \vdots\\ \mathbf{k}_{\text{mean}}\end{bmatrix}_{n_{\mathbf{K}} \times n_p}, \tag{A.7}$$

and $\mathbf{k}_{\text{mean}}$ is a row matrix of length n_p which is determined as follows:

$$\mathbf{k}_{\text{mean}} = \frac{1}{n_{\mathbf{K}}} \begin{bmatrix} \sum_{i=1}^{n_{\mathbf{K}}} (K)_{i1} & \sum_{i=1}^{n_{\mathbf{K}}} (K)_{i2} & \cdots & \sum_{i=1}^{n_{\mathbf{K}}} (K)_{in_p} \end{bmatrix}. \tag{A.8}$$

Algorithm 1 shows the Metropolis algorithm with the adaptive proposal (Eq. (A.5)).

Algorithm 1 The Metropolis algorithm with the adaptive proposal

select initial sample $\mathbf{x}_0 \in \mathbb{R}^{n_p}$ and set $\gamma = \frac{2.38}{\sqrt{n_p}}$
for $i = 0, 1, 2, ..., n_s - 1$ **do**
    draw $\mathbf{x}_p \in \mathbb{R}^{n_p}$ from the proposal distribution $q(\mathbf{x}_p|\mathbf{x}_i)$ in Eq. (A.5)
    calculate the ratio $r(\mathbf{x}_i, \mathbf{x}_p) = \min\left(1, \frac{\pi_{\text{post}}(\mathbf{x}_p)}{\pi_{\text{post}}(\mathbf{x}_i)}\right)$
    draw $u \in [0, 1]$ from uniform distribution
    if $r(\mathbf{x}_i, \mathbf{x}_p) \geq u$ **then**
        $\mathbf{x}_{i+1} = \mathbf{x}_p$
    else
        $\mathbf{x}_{i+1} = \mathbf{x}_i$
    end if
    per 1000 samples
        update matrix $\widetilde{\mathbf{K}}$
end for

Appendix B. Posterior predictive distribution

One can predict new measurements, based on the current measurements using the posterior predictive distribution. In the case in which no model uncertainties are considered, the posterior predictive distribution of new measurement y^{new}, $\pi(y^{\text{new}}|\mathbf{y}, \boldsymbol{\epsilon}, \epsilon^{\text{new}})$ results from the following integral [5]:

$$\pi(y^{\text{new}}|\mathbf{y}, \boldsymbol{\epsilon}, \epsilon^{\text{new}}) = \int_{\mathbb{R}^{n_p}} \pi(y^{\text{new}}|\mathbf{x}, \epsilon^{\text{new}}) \pi(\mathbf{x}|\mathbf{y}, \boldsymbol{\epsilon}) d\mathbf{x}, \tag{B.1}$$

where $\boldsymbol{\epsilon} = \begin{bmatrix} \epsilon_1 & \cdots & \epsilon_{n_m} \end{bmatrix}^T$ denotes the vector of measured strains, at which stresses $\mathbf{y}$ are measured. Furthermore, ϵ^{new} denotes the new strain, for which we want to predict new stress y^{new}. The integral in Eq. (B.1) can normally not be computed analytically [5]. In practise however, one can use the MCMC approach to approximate Eq. (B.1). Since we have already sampled the posterior, we can straightforwardly replace the i^{th} sample in $\pi(y^{\text{new}}|\mathbf{x}_i, \epsilon^{\text{new}})$ and then draw sample y_i^{new} from $\pi(y^{\text{new}}|\mathbf{x}_i, \epsilon^{\text{new}})$ [45]. Furthermore, the posterior mean response reads [5]:

$$\overline{y}^{\text{new}} = \int_{\mathbb{R}} y^{\text{new}} \pi(y^{\text{new}}|\mathbf{y}, \boldsymbol{\epsilon}, \epsilon^{\text{new}}) dy^{\text{new}}. \tag{B.2}$$

The integral given in Eq. (B.2) is in practise, again, approximated numerically using Monte Carlo integration. More information about posterior predictive analyses can be found in [5].

In case of model uncertainty, the posterior predictive distribution reads:

$$\pi(y^{\text{new}}|\mathbf{y}, \boldsymbol{\epsilon}, \epsilon^{\text{new}}) = \int_{\mathbb{R}^{n_d}} \int_{\mathbb{R}^{n_p}} \pi(y^{\text{new}}|\mathbf{x}, \mathbf{x}_d, \epsilon^{\text{new}}) \pi(\mathbf{x}, \mathbf{x}_d|\mathbf{y}, \boldsymbol{\epsilon}) d\mathbf{x} d\mathbf{x}_d, \tag{B.3}$$

where n_d denotes the number of parameters of the model uncertainty formulation. Note that we have assumed that the measurement noise parameters are known.

References

[1] L. A. A. Beex, C. W. Verberne, R. H. J. Peerlings, Experimental identification of a lattice model for woven fabrics: Application to electronic textile, Composites Part A: Applied Science and Manufacturing 48 (Supplement C) (2013) 82–92.

[2] L. L. Magorou, F. Bos, F. Rouger, Identification of constitutive laws for wood-based panels by means of an inverse method, Composites Science and Technology 62 (4) (2002) 591–596.

[3] K. Genovese, L. Lamberti, C. Pappalettere, Improved global-local simulated annealing formulation for solving non-smooth engineering optimization problems, International Journal of Solids and Structures 42 (1) (2005) 203–237.

[4] C. Elster, G. Wübbeler, Bayesian regression versus application of least squares-an example, Metrologia 53 (1) (2016) S10.

[5] J. L. Beck, Bayesian system identification based on probability logic, Structural Control and Health Monitoring 17 (7) (2010) 825–847.

[6] D. Higdon, H. Lee, Z. Bi, A Bayesian approach to characterizing uncertainty in inverse problems using coarse and fine scale information, IEEE Transactions on Signal Processing 50 (2002) 388–399.

[7] J. Wang, N. Zabaras, A Bayesian inference approach to the inverse heat conduction problem, International Journal of Heat and Mass Transfer 47 (17-18) (2004) 3927–3941.

[8] P. Risholm, F. Janoos, I. Norton, A. J. Golby, W. M. Wells, Bayesian characterization of uncertainty in intra-subject non-rigid registration, Medical image analysis 17 (5) (2013) 538–555.

[9] S. Lan, T. Bui-Thanh, M. Christie, M. Girolami, Emulation of higher-order tensors in manifold Monte Carlo methods for Bayesian inverse problems, Journal of Computational Physics 308 (2016) 81–101.

[10] J. Isenberg, Progressing from least squares to Bayesian estimation, in: Proceedings of the 1979 ASME design engineering technical conference, New York, 1979, pp. 1–11.

[11] K. F. Alvin, Finite element model update via Bayesian estimation and minimization of dynamic residuals, AIAA journal 35 (5) (1997) 879–886.

[12] J. L. Beck, L. S. Katafygiotis, Updating models and their uncertainties. I: Bayesian statistical framework, Journal of Engineering Mechanics 124 (4) (1998) 455–461.

[13] T. Marwala, S. Sibusiso, Finite element model updating using Bayesian framework and modal properties, Journal of Aircraft 42 (1) (2005) 275–278.

[14] T. C. Lai, K. H. Ip, Parameter estimation of orthotropic plates by Bayesian sensitivity analysis, Composite Structures 34 (1) (1996) 29–42.

[15] F. Daghia, S. de Miranda, F. Ubertini, E. Viola, Estimation of elastic constants of thick laminated plates within a Bayesian framework, Composite Structures 80 (3) (2007) 461–473.

[16] J. M. Nichols, W. A. Link, K. D. Murphy, C. C. Olson, A Bayesian approach to identifying structural nonlinearity using free-decay response: Application to damage detection in composites, Journal of Sound and Vibration 329 (15) (2010) 2995–3007.

[17] C. Gogu, W. Yin, R. Haftka, P. Ifju, J. Molimard, R. Le Riche, A. Vautrin, Bayesian identification of elastic constants in multi-directional laminate from moiré interferometry displacement fields, Experimental Mechanics 53 (4) (2013) 635–648.

[18] P. S. Koutsourelakis, A novel Bayesian strategy for the identification of spatially varying material properties and model validation: An application to static elastography, International Journal for Numerical Methods in Engineering 91 (3) (2012) 249–268.

[19] C. Gogu, R. Haftka, R. L. Riche, J. Molimard, A. Vautrin, Introduction to the Bayesian approach applied to elastic constants identification, AIAA journal 48 (5) (2010) 893–903.

[20] T. Most, Identification of the parameters of complex constitutive models: Least squares minimization vs. Bayesian updating, in: D. Straub (Ed.), Reliability and optimization of structural systems, CRC press, 2010, pp. 119–130.

[21] B. V. Rosić, A. Kčerová, J. Sýkora, O. Pajonk, A. Litvinenko, H. G. Matthies, Parameter identification in a probabilistic setting, Engineering Structures 50 (2013) 179–196, Engineering Structures: Modelling and Computations (special issue IASS-IACM 2012).

[22] M. Muto, J. L. Beck, Bayesian updating and model class selection for hysteretic structural models using stochastic simulation, Journal of Vibration and Control 14 (1-2) (2008) 7–34.

[23] P. Liu, S. K. Au, Bayesian parameter identification of hysteretic behavior of composite walls, Probabilistic Engineering Mechanics 34 (2013) 101–109.

[24] D. D. Fitzenz, A. Jalobeanu, S. H. Hickman, Integrating laboratory creep compaction data with numerical fault models: A Bayesian framework, Journal of Geophysical Research: Solid Earth 112 (B8), B08410.

[25] W. P. Hernandez, F. C. L. Borges, D. A. Castello, N. Roitman, C. Magluta, Bayesian inference applied on model calibration of fractional derivative viscoelastic model, in: V. Steffen Jr, D. A. Rade, W. M. Bessa (Eds.), DINAME 2015 - Proceedings of the XVII International symposium on dynamic problems of mechanics, Natal, 2015.

[26] H. Rappel, L. A. A. Beex, S. P. A. Bordas, Bayesian inference to identify parameters in viscoelasticity, Mechanics of Time-Dependent Materials.
URL `https://doi.org/10.1007/s11043-017-9361-0`

[27] M. C. Kennedy, A. O'Hagan, Bayesian calibration of computer models, Journal of the Royal Statistical Society: Series B (Statistical Methodology) 63 (3) (2001) 425–464.

[28] D. Higdon, J. Gattiker, B. Williams, M. Rightley, Computer model calibration using high-dimensional output, Journal of the American Statistical Association 103 (482) (2008) 570–583.

[29] J. McFarland, S. Mahadevan, Multivariate significance testing and model calibration under uncertainty, Computer Methods in Applied Mechanics and Engineering 197 (29) (2008) 2467–2479.

[30] G. B. Arhonditsis, D. Papantou, W. Zhang, G. Perhar, E. Massos, M. Shi, Bayesian calibration of mechanistic aquatic biogeochemical models and benefits for environmental management, Journal of Marine Systems 73 (1) (2008) 8–30.

[31] S. Sankararaman, Y. Ling, C. Shantz, S. MahadevaA, Inference of equivalent initial flaw size under multiple sources of uncertainty, International Journal of Fatigue 33 (2) (2011) 75–89.

[32] P. D. Arendt, D. W. Apley, W. Chen, Quantification of model uncertainty: Calibration, model discrepancy, and identifiability, Journal of Mechanical Design 134 (10) (2012) 100908.

[33] K. V. Yuen, L. S. Katafygiotis, Bayesian modal updating using complete input and incomplete response noisy measurements, Journal of Engineering Mechanics 128 (3) (2002) 340–350.

[34] S. F. Gull, Bayesian data analysis: Straight-line fitting, in: J. Skilling (Ed.), Maximum entropy and Bayesian methods, Vol. 36 of Fundamental Theories of Physics, Springer Science & Business Media, Netherlands, 1989, pp. 511–518.

[35] P. Dellaportas, D. A. Stephens, Bayesian analysis of errors-in-variables regression models, Biometrics 51 (3) (1995) 1085–1095.

[36] R. J. Carroll, K. Roeder, L. Wasserman, Flexible parametric measurement error models, Biometrics 55 (1) (1999) 44–54.

[37] R. Scheines, H. Hoijtink, A. Boomsma, Bayesian estimation and testing of structural equation models, Psychometrika 64 (1) (1999) 37–52.

[38] B. C. Kelly, Some aspects of measurement error in linear regression of astronomical data, The Astrophysical Journal 665 (2) (2007) 1489.

[39] D. W. Hogg, J. Bovy, D. Lang, Data analysis recipes: Fitting a model to data, ArXiv e-prints`arXiv:1008.4686`.

[40] Y. Ling, J. Mullins, S. Mahadevan, Selection of model discrepancy priors in bayesian calibration, Journal of Computational Physics 276 (Supplement C) (2014) 665–680.

[41] Y. Xiong, W. Chen, K.-L. Tsui, D. W. Apley, A better understanding of model updating strategies in validating engineering models, Computer Methods in Applied Mechanics and Engineering 198 (15) (2009) 1327–1337.

[42] J. Brynjarsdóttir, A. O'Hagan, Learning about physical parameters: The importance of model discrepancy, Inverse Problems 30 (11) (2014) 114007.

[43] H. Haario, E. Saksman, J. Tamminen, Adaptive proposal distribution for random walk Metropolis algorithm, Computational Statistics 14 (3) (1999) 375–396.

[44] C. E. Rasmussen, C. K. Williams, Gaussian processes for machine learning, Vol. 1, MIT press Cambridge, 2006.

[45] W. R. Gilks, S. Richardson, D. Spiegelhalter, Markov chain Monte Carlo in practice, CRC press, 1995.

[46] S. Hassani, Mathematical methods: For students of physics and related fields, Springer Science & Business Media, New York, 2008.

[47] S. Brooks, A. Gelman, G. Jones, X. L. Meng, Handbook of Markov chain Monte Carlo, CRC press, 2011.

[48] A. Gelman, G. O. Roberts, W. R. Gilks, Efficient Metropolis jumping rules, in: J. M. Bernardo, J. O. Berger, A. P. Dawid, A. F. M. Smith (Eds.), Bayesian statistics, Vol. 5 of Oxford Sci. Publ., Oxford University Press, New York, 1996, pp. 599–607.

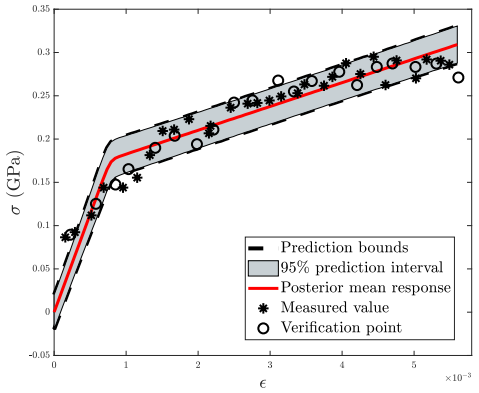

(a) Error in the stress only

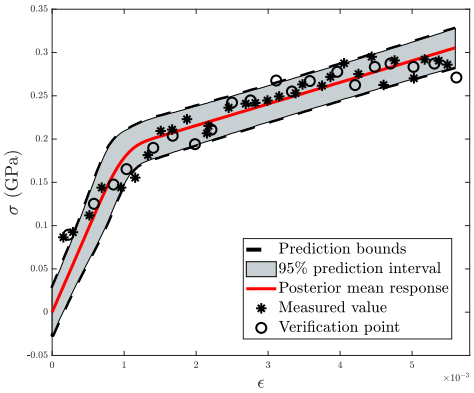

(b) Error in both the stress and the strain

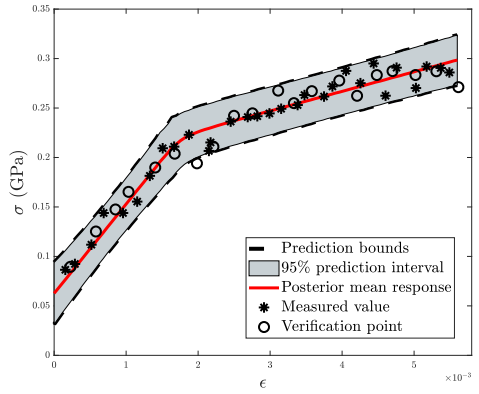

(c) Normal distribution with constant parameters

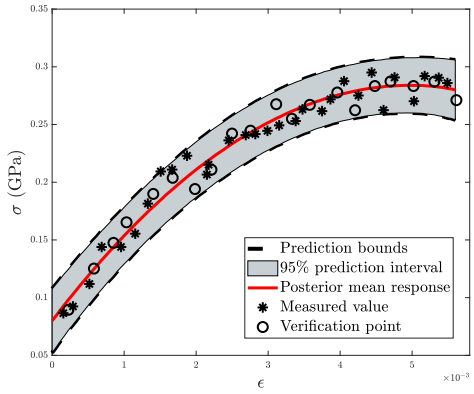

(d) Normal distribution with an input-dependent mean

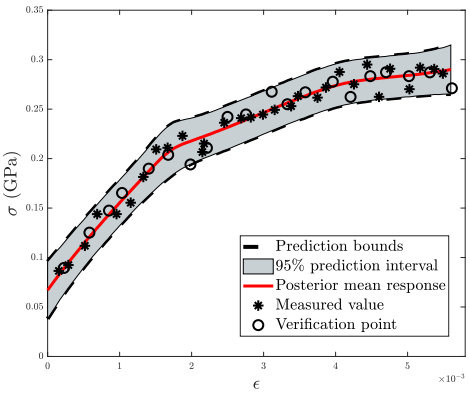

(e) Gaussian process

Figure 7: Linear elasticity-linear hardening: The measurements, the verification points, the posterior mean responses and the posterior predictions. Note that for all cases in which model uncertainty is incorporated, the error in the strain is also incorporated. One can see that considering model uncertainty results in more measurements to be present inside the bounds of the posterior predictions. For the cases in which model uncertainty is input-dependent the model uncertainty is so dominant that the two linear regimes in the model response (the elastic regime and the elastoplastic regime) cannot be recognised anymore.

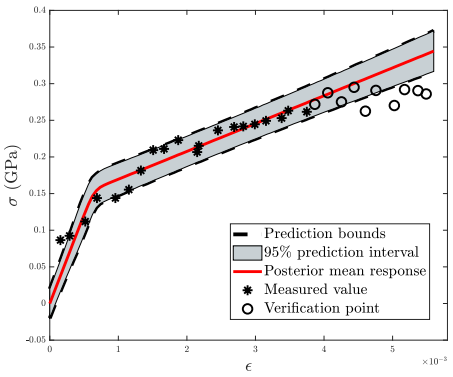

(a) Error in the stress only

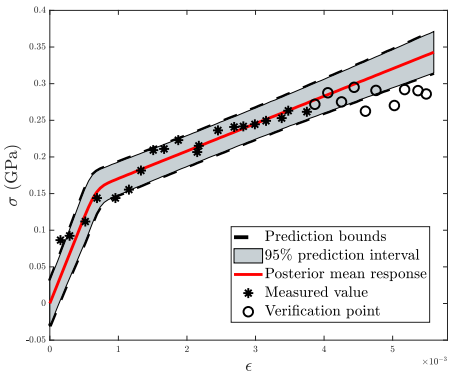

(b) Error in both the stress and the strain

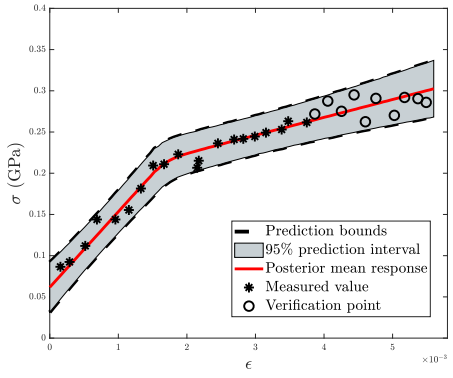

(c) Normal distribution with constant parameters

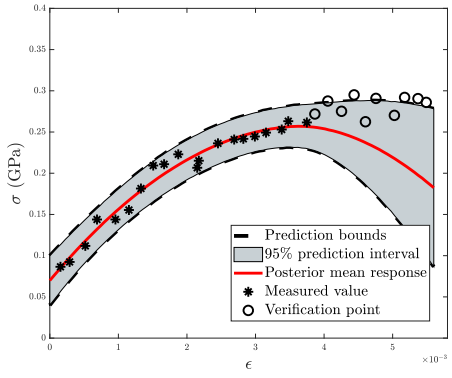

(d) Normal distribution with an input-dependent mean

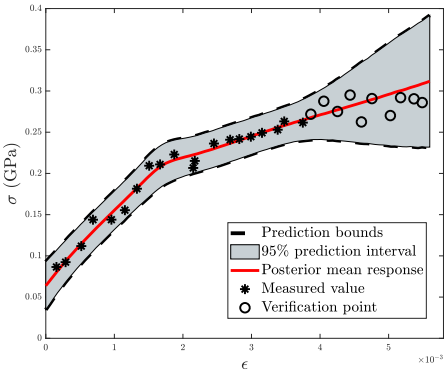

(e) Gaussian process

Figure 8: Linear elasticity-linear hardening: The measurements, the verification points, the posterior mean responses and the posterior predictions. Note that for all cases in which model uncertainty is incorporated, the error in the strain is also incorporated. One can see that considering model uncertainty results in more measurements to be located inside the bounds of the posterior predictions. It can be observed that all verification data are inside the posterior predictions' bounds if model uncertainty is described by a random variable coming from a normal distribution with constant parameters or by a Gaussian process. In case model uncertainty is described by a Gaussian process furthermore, the uncertainty is substantially larger than if a random variable coming from a normal distribution with constant parameters is used. This can be due to the fact that the Gaussian process assumes the measurements to be correlated, and hence, the larger the distance from the measured data, less information is available and a larger spread is observed. It can furthermore be observed that the smallest number of verification data is present inside the posterior prediction's bounds if model uncertainty is represented by a normal distribution with an input-dependent mean. It must be noted though, that if another relation for the mean would be selected, the posterior predictions would differ.